

Organometal Halide Perovskites as Visible-Light Sensitizers for Photovoltaic Cells

Akihiro Kojima,[†] Kenjiro Teshima,[‡] Yasuo Shirai,[§] and Tsutomu Miyasaka^{*,†,‡,||}

Graduate School of Arts and Sciences, The University of Tokyo, 3-8-1 Komaba, Meguro-ku, Tokyo 153-8902, Japan, Graduate School of Engineering, Toin University of Yokohama, and Peccell Technologies, Inc., 1614 Kurogane-cho, Aoba, Yokohama, Kanagawa 225-8502, Japan, and Graduate School of Engineering, Tokyo Polytechnic University, 1583 Iiyama, Atsugi, Kanagawa 243-0297, Japan

Received December 9, 2008; Revised Manuscript Received April 1, 2009; E-mail: miyasaka@cc.toin.ac.jp

Light-energy conversion by photoelectrochemical cells has been extensively studied in the past 50 years using various combinations of inorganic semiconductors and organic sensitizers.¹ Dye-sensitized mesoscopic TiO₂ films have been established as high-efficiency photoanodes for solar cells.² As cost-effective devices, dye-sensitized photovoltaic cells suit vacuum-free printing processes for cell fabrication; such processes enable researchers to design thin, flexible plastic cells by low-temperature TiO₂ coating technology.³ With a thin photovoltaic film, optical management is an important key for harvesting light while ensuring high efficiency. Organic sensitizers often limit light-harvesting ability because of their low absorption coefficients and narrow absorption bands. To overcome this, researchers have examined quantum dots such as CdS,^{4a,b} CdSe,^{4c–e} PbS,^{4f,g} InP,^{4h} and InAs⁴ⁱ for photovoltaic cells in both electrochemical and solid-state structures. Intense band-gap light absorption by these inorganic sensitizers, however, has not allowed high performance in quantum conversion and photovoltaic generation; significant losses in light utilization and/or charge separation are found at the semiconductor–sensitizer interface. We have studied the photovoltaic function of the organic–inorganic lead halide perovskite compounds CH₃NH₃PbBr₃ and CH₃NH₃PbI₃ as visible-light sensitizers in photoelectrochemical cells. In addition to being synthesized from abundant sources (Pb, C, N, and halogen), these perovskite materials have unique optical properties,⁵ excitonic properties,⁶ and electrical conductivity.⁷ In this report, we show a photovoltaic function of the perovskite nanocrystalline particles self-organized on TiO₂ as n-type semiconductors. Solar energy was converted with an efficiency of 3.8% on a CH₃NH₃PbI₃-based cell, while a high photovoltage of 0.96 V was obtained with a CH₃NH₃PbBr₃-based cell.

Each photoelectrode was prepared on a fluorine-doped SnO₂ transparent conductive glass (FTO, 10 Ω/sq, Nippon Sheet Glass) as a substrate, the surface of which had been pretreated by soaking in a 40 mM TiCl₄ aqueous solution at 70 °C for 30 min to form a thin TiO₂ buffer layer. A mesoporous film of TiO₂ (n-type semiconductor) was prepared on the above-treated FTO by coating with a commercial nanocrystalline TiO₂ paste (see the Supporting Information) using a screen printer and sintering at 480 °C for 1 h in air. The resultant TiO₂ film had a thickness of 8–12 μm. Nanocrystalline particles of CH₃NH₃PbX₃ (X = Br, I) were deposited on the TiO₂ surface by a self-organization process starting with the coating of a precursor solution containing stoichiometric amounts of CH₃NH₃X and PbX₂. CH₃NH₃Br and CH₃NH₃I were synthesized from HBr and HI, respectively, by reaction with 40%

methylamine in methanol solution followed by recrystallization. Synthesis of CH₃NH₃PbBr₃ on the TiO₂ surface was carried out by dropping onto the TiO₂ film a 20 wt % precursor solution of CH₃NH₃Br and PbBr₂ in *N,N*-dimethylformamide; subsequent film formation was done by spin-coating.⁸ For CH₃NH₃PbI₃, an 8 wt % precursor solution of CH₃NH₃I and PbI₂ in γ -butyrolactone was employed. The liquid precursor film coated on the TiO₂ gradually changed color simultaneously with drying, indicating the formation of CH₃NH₃PbX₃ in the solid state. A vivid color change from colorless to yellow occurred for CH₃NH₃PbBr₃ and from yellowish to black for CH₃NH₃PbI₃. X-ray diffraction analysis (Rigaku RINT-2500) for CH₃NH₃PbBr₃ and CH₃NH₃PbI₃ prepared on TiO₂ showed that both materials have crystalline structures that can be assigned to the perovskite form. CH₃NH₃PbBr₃ gave diffraction peaks at 14.77, 20.97, 29.95, 42.9, and 45.74°, assigned as the (100), (110), (200), (220), and (300) planes, respectively, of a cubic perovskite structure with a lattice constant of 5.9 Å.⁹ CH₃NH₃PbI₃ gave peaks at 14.00 and 28.36° for the (110) and (220) planes, respectively, of a tetragonal perovskite structure with *a* = 8.855 Å and *c* = 12.659 Å.⁹ Scanning electron microscopy (SEM) observation of the CH₃NH₃PbBr₃-deposited TiO₂ showed nanosized particles (2–3 nm) that existed here and there on the TiO₂ and/or CH₃NH₃PbBr₃ surface (Figure 1).

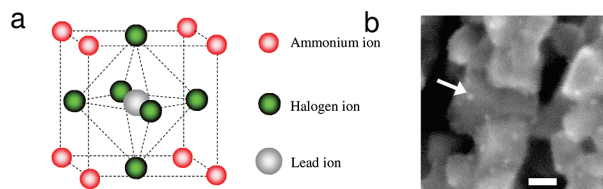


Figure 1. (a) Crystal structures of perovskite compounds. (b) SEM image of particles of nanocrystalline CH₃NH₃PbBr₃ deposited on the TiO₂ surface. The arrow indicates a particle, and the scale bar shows 10 nm.

A photovoltaic cell was constructed by combining the CH₃NH₃PbX₃-deposited TiO₂ electrode (CH₃NH₃PbX₃/TiO₂) as the photoelectrode (anode) and a Pt-coated FTO glass as the counter electrode (cathode) with insertion of a 50 μm thick separator film. The gap between the electrodes was filled with an organic electrolyte solution containing lithium halide and halogen as a redox couple; the CH₃NH₃PbBr₃/TiO₂-based cell employed an electrolyte consisting of 0.4 M LiBr and 0.04 M Br₂ dissolved in acetonitrile, while the CH₃NH₃PbI₃/TiO₂-based cell employed 0.15 M LiI and 0.075 M I₂ dissolved in methoxyacetonitrile. A sandwich-type open cell had an effective light-exposure area of 0.238 cm² with the use of a black mask. Incident photon-to-current quantum conversion efficiency (IPCE) and photocurrent–voltage (*I*–*V*) performance were measured on an action spectrum measurement setup (PEC-S20) and

[†] The University of Tokyo.[‡] Peccell Technologies, Inc.[§] Tokyo Polytechnic University.^{||} Toin University of Yokohama.

a solar simulator (PEC-L10, Pecell Technologies), respectively, the latter irradiating simulated sunlight of AM 1.5 and 100 mW/cm² intensity.

Light irradiation of the photocells caused generation of anodic photocurrents with amplitudes of 5–11 mA/cm². After optimization of the average TiO₂ thickness for short-circuit photocurrent density (J_{sc}), the maximum J_{sc} occurred with 8 μ m for CH₃NH₃PbI₃/TiO₂ and 12 μ m for CH₃NH₃PbBr₃/TiO₂. Figure 2a compares action spectra of the IPCE for the photocells based on CH₃NH₃PbBr₃/TiO₂ and CH₃NH₃PbI₃/TiO₂. With CH₃NH₃PbBr₃/TiO₂, the photocurrent occurred in the visible wavelength region ($\lambda < 600$ nm). The IPCE exhibited a sharp rise at ~ 570 nm with saturation at < 520 nm, which is characteristic of band-gap absorption. With a maximum of 65%, a plateau of IPCE indicates that incident photons are strongly absorbed by the 8 μ m thin film of CH₃NH₃PbBr₃/TiO₂. The perovskite iodide, CH₃NH₃PbI₃/TiO₂, resulted in a low IPCE (45%) but showed an extended spectral responsivity to $\lambda = 800$ nm, reflecting the black color of the electrode. This bathochromic shift by halogen substitution⁶ is analogous to that for silver halide ionic crystals. The anodic photocurrent with high IPCE values corroborates that TiO₂ was efficiently sensitized by the nanocrystalline perovskite. Work function analysis by photoelectron spectroscopy of spin-coated polycrystalline films showed valence-band levels of CH₃NH₃PbBr₃ and CH₃NH₃PbI₃ at ~ 5.38 and 5.44 eV versus the vacuum level, respectively (see the Supporting Information). Electrochemically, these valence-band levels are considered to be more positive than the oxidation potentials of the corresponding halides in the electrolyte, which, depending on halide concentration, are estimated to be 5.1–5.6 eV for Br₂/Br[−] and 4.5–5.0 eV for I₂/I[−]. The conduction-band levels calculated from the wavelengths of the optical absorption edges are at ~ 3.36 and 4.0 eV for CH₃NH₃PbBr₃ and CH₃NH₃PbI₃, respectively; such values allow electron injection to the TiO₂ conduction band (~ 4.0 eV). As for the quantum confinement effect, the IPCE spectra show that it may not dominate the present perovskite system if it partially exists by sensitizing TiO₂ at shorter wavelengths.

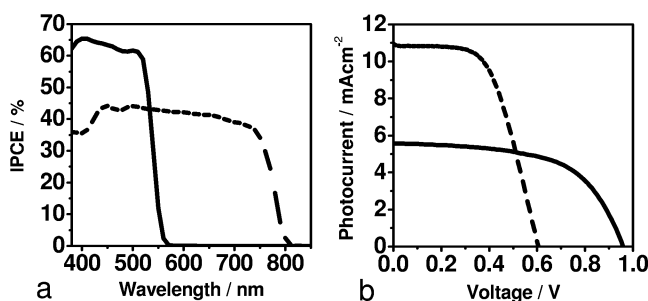


Figure 2. (a) IPCE action spectra for photoelectrochemical cells using CH₃NH₃PbBr₃/TiO₂ (solid line) and CH₃NH₃PbI₃/TiO₂ (dashed line). (b) Photocurrent–voltage characteristics for cells using CH₃NH₃PbBr₃/TiO₂ (solid line) and CH₃NH₃PbI₃/TiO₂ (dashed line) under 100 mW cm^{−2} AM 1.5 irradiation.

Figure 2b and Table 1 show the I – V characteristics of the CH₃NH₃PbBr₃ and CH₃NH₃PbI₃-sensitized photovoltaic cells under exposure to 100 mW cm^{−2} AM 1.5 simulated sunlight. The J_{sc} value, which reflects the integrated area of the IPCE, was much larger for the CH₃NH₃PbI₃-sensitized cell than for CH₃NH₃PbBr₃ cell, the former yielding $J_{sc} = 11$ mA/cm², twice that of the latter. In contrast, the CH₃NH₃PbI₃-sensitized cell showed a low open-circuit voltage (V_{oc}) of 0.61 V, while the CH₃NH₃PbBr₃-sensitized cell yielded a notably high V_{oc} of 0.96 V. The high V_{oc} of the bromide (CH₃NH₃PbBr₃) is associated with the higher conduction band of the bromide relative to that of the iodide. This implies that

the perovskite sensitizer electronically interacts with the surface conduction-band levels of TiO₂ that have distribution between particles. With Ru complex sensitizers and TiO₂, the maximal V_{oc} ever reported is in the range 0.86–0.93 V.¹⁰ We assume that the origin of the high V_{oc} is the bromide employed as a redox partner to couple with the perovskite bromide; the electrochemically more positive potential of bromide compared with iodide expands the range of photovoltage. As a result, however, the highest power conversion efficiency (η) of 3.81% was obtained with the iodide (CH₃NH₃PbI₃) backed by the high IPCE and J_{sc} . This efficiency is significantly higher than those obtained to date with nonorganic sensitizers and quantum dots.^{4a–i} In studies of durability, continuous irradiation caused a photocurrent decay for an open cell exposed to air; this mechanism needs more study to improve the cell lifetime.

Table 1. Photovoltaic Characteristics of Perovskite-Based Cells^a

perovskite sensitizer on TiO ₂	J_{sc} (mA/cm ²)	V_{oc} (V)	FF	η (%)
CH ₃ NH ₃ PbBr ₃	5.57	0.96	0.59	3.13
CH ₃ NH ₃ PbI ₃	11.0	0.61	0.57	3.81

^a Measured with an effective incident area of 0.24 cm² under 100 mW/cm² AM 1.5 simulated sunlight irradiation.

In conclusion, the organolead halide perovskite compounds efficiently sensitize TiO₂ for visible-light conversion in photovoltaic cells. The materials are especially promising for realizing high photovoltages close to 1.0 V. A series of organic–inorganic perovskite materials CH₃NH₃MX₃ (M = Pb, Sn; X = halogen) exhibiting different energy gaps⁵ are also targets for optimizing the cell performance.

Acknowledgment. This work was supported by a Grant-in-Aid for Science from the Ministry of Education, Culture, Sports, Science, and Technology, Japan. We thank Professor H. Segawa of The University of Tokyo for work function measurements.

Supporting Information Available: Preparation of TiO₂ materials, color of the perovskite compounds, and work function analysis for the perovskite crystals. This material is available free of charge via the Internet at <http://pubs.acs.org>.

References

- (1) Memming, R. *Semiconductor Electrochemistry*; Wiley-VCH: Weinheim, Germany, 2001.
- (2) Chiba, Y.; Islam, A.; Watanabe, Y.; Komiya, R.; Koide, N.; Han, L. *Jpn. J. Appl. Phys.* **2006**, *45*, L638–L640. Gao, F.; Wang, Y.; Shi, D.; Zhang, J.; Wang, M.; Jing, X.; Humphry-Baker, R.; Wang, P.; Zakeeruddin, S. M.; Grätzel, M. *J. Am. Chem. Soc.* **2008**, *130*, 10720–10728.
- (3) Miyasaka, T.; Kijitori, Y.; Murakami, T. N.; Kimura, M.; Uegusa, S. *Chem. Lett.* **2002**, 1250–1251. Miyasaka, T.; Ikegami, M.; Kijitori, Y. *J. Electrochem. Soc.* **2007**, *154*, A455–A461. Ikeda, N.; Miyasaka, T. *Chem. Lett.* **2007**, *36*, 466–467.
- (4) (a) Tachibana, Y.; Akiyama, H. Y.; Ohtsuka, Y.; Torimoto, T.; Kuwabata, S. *Chem. Lett.* **2007**, *36*, 88–89. (b) Chang, C. H.; Lee, Y. L. *Appl. Phys. Lett.* **2007**, *91*, 053503. (c) Robel, I.; Subramanian, V.; Kuno, M.; Kamat, P. V. *J. Am. Chem. Soc.* **2006**, *128*, 2385–2393. (d) Niitsoo, O.; Sarkar, S. K.; Pejoux, C.; Ruhle, S.; Cahen, D.; Hodes, G. *J. Photochem. Photobiol., A* **2006**, *181*, 306–313. (e) Diguna, L. J.; Shen, Q.; Kobayashi, J.; Toyoda, T. *Appl. Phys. Lett.* **2007**, *91*, 023116. (f) Plass, R.; Pelet, S.; Krueger, J.; Grätzel, M.; Bach, U. *J. Phys. Chem. B* **2002**, *106*, 7578–7580. (g) Hoyer, P.; Könenkamp, R. *Appl. Phys. Lett.* **1995**, *626*, 349–351. (h) Zaban, A.; Micic, O. I.; Gregg, B. A.; Nozik, A. J. *Langmuir* **1998**, *14*, 3153–3156. (i) Yu, P.; Zhu, K.; Norman, A. G.; Ferrere, S.; Frank, A. J.; Nozik, A. J. *J. Phys. Chem. B* **2006**, *110*, 25451–25454.
- (5) Papavassiliou, G. C. *Mol. Cryst. Liq. Cryst.* **1996**, *286*, 231–238.
- (6) Tanaka, K.; Takahashi, T.; Ban, T.; Kondo, T.; Uchida, K.; Miura, N. *Solid State Commun.* **2003**, *127*, 619–623.
- (7) Yamada, K.; Kawaguchi, H.; Matsui, T.; Okuda, T.; Ichiba, S. *Bull. Chem. Soc. Jpn.* **1990**, *63*, 2521–2525.
- (8) Kitazawa, N.; Watanabe, Y.; Nakamura, Y. *J. Mater. Sci.* **2002**, *37*, 3585–3587.
- (9) Poglitsch, A.; Weber, D. *J. Chem. Phys.* **1987**, *87*, 6373–6378.
- (10) Henry, J.; Snaith, A. J.; Moule, C. K.; Meerholz, K.; Friend, R. H.; Grätzel, M. *Nano Lett.* **2007**, *7*, 3372–3376.

JA809598R